CD62L as target receptor for specific gene delivery into less differentiated human T lymphocytes

Laura Kapitza¹, Naphang Ho¹, Thomas Kerzel¹, Annika Frank M¹, Frederic Thalheimer B¹, Thomas Schaser², Christian Buchholz¹, and Jessica Hartmann¹

¹Paul-Ehrlich-Institut ²Miltenyi Biotec BV & Co KG

September 27, 2022

Abstract

Chimeric antigen receptor (CAR) expressing T cells are a complex and heterogeneous gene therapy product with variable phenotype composition. A higher proportion of less differentiated CAR T cells is usually associated with improved antitumoral function and persistence. We describe here a novel receptor-targeted lentiviral vector (LV), named 62L-LV, that preferentially transduces less differentiated T cells marked by the L-selectin receptor CD62L, with transduction rates of up to 70% of CD4 $^+$ and 50% of CD8 $^+$ primary T cells. Remarkably, higher amounts of less differentiated T cells are transduced and preserved upon long-term cultivation using 62L-LV compared to VSV-LV. Interestingly, shed CD62L neither altered binding of 62L-LV particles to T cells nor impacted their transduction. Incubation of two days activated T lymphocytes with 62L-LV or VSV-LV for only 24 hours was sufficient to generate CAR T cells that controlled tumor growth in an NSG mouse model. The data prove that potent CAR T cells can be generated by short-term *ex vivo* exposure of primary cells to LVs. As a first vector type that preferentially transduces less differentiated T lymphocytes, 62L-LV has the potential to circumvent cumbersome selection of T cell subtypes and offers substantial shortening of the CAR T cell manufacturing process.

Introduction

Genetic modification of T cells to express a chimeric antigen receptor (CAR) has emerged as an effective therapeutic treatment for patients with B cell hematological malignancies over the last years. CAR T cells are generated from peripheral T cells isolated from blood of patients. Based on the differential expression of CD62L, CCR7, CD45RA and CD45RO, these peripheral T cells can be divided into five subsets: naive T (T_N) cells, which are antigen-unexperienced, effector T (T_{EFF}) cells, which migrate to sites of inflammation and promote pathogen clearance, and memory T cells, which persist long-term to allow protection against subsequent infections. Memory T cells include stem cell memory (T_{SCM}) , central memory (T_{CM}) and effector memory (T_{EM}) cells. In humans, T cell differentiation follows a linear progression where less differentiated cells give rise to more differentiated progeny: $T_N > T_{SCM} > T_{CM} > T_{EM} > T_{EFF}$. During differentiation of T_N towards T_{EFF} cells, the proliferative potential and memory functions are declining, while effector functions increase. Notably, the two markers, CD62L and CCR7 are only expressed on T_N and early differentiated $(T_{SCM} \text{ and } T_{CM})$ cells. During T cell isolation and subsequent cultivation, cells are usually activated using cytokines and stimulating antibodies to induce T cell proliferation and survival. In the past, IL-2 was most frequently used for cytokine support, thereby driving T cell cultures towards terminally differentiated T cells. More recently, IL-7 and IL-15 are applied for T cell cultures in an effort to maintain a more naïve- or memory-like T cell phenotype.

Despite its promising results, CAR T cell therapy still needs to overcome various hurdles to become standard therapy for all patients in need. Automated processes have been developed to address the complicated manufacturing process. However, the most suitable T cell phenotype for CAR-mediated tumor therapy is a matter of debate. In general, naive and early memory T cells, are favored for cellular immunotherapy products due to their higher plasticity, longer persistence and greater capability to proliferate and differentiate into highly cytolytic effector cells. Along this line, a beneficial antitumoral function and cell persistence was associated with a high amount of less differentiated CAR T cells not only in patients with B-cell malignancies but also in patients with neuroblastoma.

For the generation of CAR T cell products, lentiviral vectors (LVs) pseudotyped with the glycoprotein of the vesicular stomatitis virus (VSV-G), harboring a broad tropism, are commonly used. Optimizing gene delivery through engineering of vector particles offers the potential to improve and simplify genetic modification of T cells. In this regard, receptor-targeted LVs (RT-LVs) specifically transducing CD3, CD4 or CD8 T cells have been described. All three vector types were recently shown to mediate the generation of CAR T cells directly *in vivo* in humanized mouse models. RT-LVs use a cell surface protein of choice as entry receptor, which can be achieved through pseudotyping with engineered glycoproteins from paramyxoviruses displaying a receptor-specific targeting domain, such as a single-chain antibody fragment (scFv) or designed ankyrin repeat molecule (DARPin). However, the T cell specific LVs available so far do not discriminate between the differentiation phenotype and exhaustion status of T cells.

Here we describe the generation of a RT-LV that is specific for a T cell marker expressed on less differentiated T cells: CD62L. The specificity of this vector was mediated by displaying a CD62L-specific scFv on measles virus (MV)-based RT-LVs. The resulting CD62L-LV mediated efficient gene delivery and preserved a higher degree of less differentiated CAR T cells upon long-term culture. CAR T cells generated through short-term incubation with CD62L-LV controlled tumor burden in an *in vivo* setting.

Results

A CD62L-specific scFv was derived from the antibody clone 145/15. Its sequence was fused to either the MV H protein or the NiV G protein, to the latter via a short and a long $[(G_4S)_3]$ linker (L3). All three constructs were equally well expressed at the surface of transfected HEK-293T cells (Suppl. Fig. 1). For production of CD62L-targeted LVs, HEK-293T producer cells were transfected with two envelope plasmids (one encoding MV H or NiV G fused to the targeting moiety, the other the fusion protein MV F or NiV F), the lentiviral packaging plasmid and the transfer vector encoding gfp. Vector particles harvested as unconcentrated supernatant were used for transduction of target cells (HT1080_{CD62L} and HT1080_{α Hic}) and non-target cells (HT1080). Notably, HT1080_{α Hic} cells are applicable target cells due to the presence of a His-tag at the C-terminal part of the CD62L-scFv fused to the NiV G and MV H protein.

While ^{MV-L3}62L-LV was highly active in transducing both target cell types, both NiV glycoprotein-based LVs were inefficient in gene delivery, especially on HT1080_{CD62L} cells (Suppl. Fig. 2). Hence, ^{MV-L3}62L-LV (hereafter called 62L-LV) was chosen for further investigation. For all following experiments, a second generation α CD19-CAR covering the 4-1BB costimulatory domain and the CD3 ζ -signaling domain as well as a truncated LNGFR (Δ LNGFR) reporter protein was packaged into LV particles. This vector was produced at large scale, purified and concentrated over a sucrose cushion. Vector stocks contained 2.6 – 7.9x10¹¹ particles/mL, which were on average 142 ± 7 nm in size (Fig. 1A). Transduction efficiency was even higher on primary human PBMC than on HT1080_{αHtc} cells (Fig. 1B). CAR gene delivery was strictly dependent on CD62L expression, since 62L-LV transduced HT1080_{CD62L} cells, but not the parental HT1080 cells (Fig. 1C).

Transduction of activated primary human PBMC obtained from various donors resulted in efficient gene transfer into $CD4^+$ and $CD8^+$ T lymphocytes (Fig. 2A). Gene transfer rates were substantially enhanced by the addition of Vectofusin-1, resulting in more than 70% $CD4^+CAR^+$ T cells and 50% $CD8^+CAR^+$ T cells.

They were thus comparable to those obtained with VSV-LV (Fig. 2A and Suppl. Fig. 3). Interestingly, even after cultivation of these cells for several days, CAR T cells generated with 62L-LV contained significantly higher numbers of less differentiated cells than CAR T cells generated with VSV-LV, as indicated by the higher percentage of $CD62L^+$ cells (Fig. 2B).

To demonstrate specificity of 62L-LV on primary human PBMC, a blocking experiment with the parental CD62L antibody (145/15) or an unrelated antibody against CD45 was performed. Incubation of activated PBMC with increasing concentrations of either anti-CD62L or anti-CD45 resulted in a gradual increase in cell staining intensity for both antibodies (Fig. 3A). CD62L staining peaked at a concentration of 2.2 ng/mL while for anti-CD45 saturation was only about to be reached for the highest concentration applied, although 100% of the cells were positive for CD45 also at lower antibody concentrations (Fig. 3A and Suppl. Fig. 4). Addition of 62L-LV vector particles to antibody pre-incubated cells showed that 62L-LV particle binding to cells decreased with increasing concentrations of anti-CD62L, while the unrelated antibody CD45 did not influence vector binding (Fig. 3B). Notably, vector binding onto PBMC could be reduced close to background levels already at an anti-CD62L concentration of 2.2 ng/mL, demonstrating that 62L-LV binds specifically to CD62L on primary cells.

During T cell activation and differentiation, CD62L is shed from the T cell surface. This has two consequences. First, CD62L levels on T cells are strongly fluctuating in cell culture. It is therefore difficult to correlate CAR gene and CD62L expression to prove the selectivity of 62L-LV after transduction of primary human PBMC. Second, shed CD62L (sCD62L) may bind to vector particles and reduce their gene transfer activity. Whether sCD62L hinders transduction by sequestering vector particles was subsequently analyzed in a binding experiment. As expected, accumulation of sCD62L in the supernatant of activated PBMC was observed for up to 10 days (Fig. 4A). Supernatant from day six, containing on average 64 ng/mL sCD62L, was used to pre-incubate 62L-LV particles prior to T cell binding. Interestingly, pre-incubation of 62L-LV with either fresh or frozen supernatants containing sCD62L did not influence binding of the vector particles to PBMC. Similar staining intensities of the reporter protein were detected regardless whether vector particles were incubated with sCD62L containing supernatants or fresh medium, indicating that sCD62L molecules present in cell culture supernatants did not alter binding of 62L-LV to T cells (Fig. 4B). Along this line, pre-incubation of vector and sCD62L did not impact the transduction efficiency of 62L-LV particles (Suppl. Fig. 5).

After having demonstrated that 62L-LV can specifically transfer CAR genes into the genome of CD62Lpositive T cells, we investigated the functionality of those CAR T cells in an *in vivo* setting compared to CAR T cells generated with a conventional VSV-G pseudotyped LV. CAR T cells were short term generated within 3 days by 24h incubation of activated PBMC with either 62L-LV or VSV-LV and subsequently administered to NSG mice via tail vein injection. Notably, a higher amount of vector bound T cells were present in the infused product of 62L-LV-treated T cells compared to VSV-LV-treated ones, refelecting that 1.3-fold more vector particles were applied in the 62L-LV group (Suppl. Fig. 6). Untransduced PBMC served as control. To demonstrate their functionality, Nalm6 cells (luciferase-encoding CD19-positive target cells) were intravenously injected into the mice three days later and tumor growth was followed by bioluminescence imaging (BLI). A schematic time line of the experimental set-up is presented in Figure 5A. Tumor growth was clearly constrained in both vector groups, while a steady increase of tumor mass, reflected by a more than 100-fold increase in luciferase signal, was observed in all control animals (Fig. 5B). Quantification of signals revealed that tumor load in both vector groups remained at or slightly above the background level over all days of analysis (Fig. 5C). Notably, signals in animals that received VSV-LV-treated T cells were slightly reduced compared to those receiving 62L-LV-treated cells, but this difference was not significant. At day 17 post-adoptive cell transfer, no tumor cells were detected in blood, bone marrow, liver and spleen of the sacrificed mice of both vector groups, while tumor cells were present in various organs of all control animals (Fig. 5D). Along this line, proliferation of CAR T cells was observed in blood over time of animals having received 62L-LV- or VSV-LV-incubated PBMC (Fig. 6A). Interestingly, a higher proportion of CAR T cells and human CD45+ cells in general was observed for the VSV-LV group in spleen, blood and bone marrow at day 17 (Fig. 6B-D). Similar trend was observed for liver as well (Fig. 6E). These finding might

reflect the fact that a nearly 6.5-fold increased MOI was used for PBMC transduction in the VSV-LV group. In conclusion, in the applied animal model functional CAR T cells can be generated with 62L-LV by short term*ex vivo* exposure to vector particles, which are similarly potent as VSV-LV derived CAR T cells.

Discussion

For any CAR T cell therapy, generating a product with high safety and efficacy in terms of longevity, engraftment and antitumor-effector function is the ultimate goal. CAR T cell design and cellular composition of the CAR T cell product are essential parameters defining these key therapeutic features. Parameters affecting CAR T cell function are e.g. the choice of costimulation, ratio between CD4⁺ and CD8⁺ CAR T cells, CAR T cell differentiation status and amount of exhausted CAR T cells. This paper describes a novel gene transfer vector, termed 62L-LV, which specifically transduces CD62L-positive cells, thus offering the potential to preferentially generate $CD62L^+$ CAR T cells without the need of preselection of defined T cell subsets. Importantly, the newly generated 62L-LV vector could be robustly produced with regard to particle size, concentration and functional titer. With an average size of 142 nm and 10^{11} particles/mL, size and concentrations of 62L-LV stocks lay in the expected ranges of previously established RT-LVs. Functional titers of concentrated 62L-LV batches encoding the α CD19-CAR were on average above 1×10^6 t.u./mL on $HT1080_{\alpha Hic}$ cells and about one log higher on PBMC. This difference in gene transfer activity illustrates that titer determination depends on the particular experimental conditions including the cell type, used transgene and transduction condition. Functional titers can therefore not be compared to those of other vector types. Gene transfer into primary human PBMC with 62L-LV was as efficient as with VSV-LV using same amount of vector volume (Suppl. Fig. 3), yet still resulted in a significantly higher proportion of less differentiated CAR T cells upon long term cultivation.

As CD62L is a T cell differentiation marker, its expression changes throughout T cell life time and activation status. CD62L is regulated by transcriptional shutdown of the CD62L gene as well as shedding from the cell surface upon T cell activation. Therefore, direct proof for the selectivity of 62L-LV on primary cells is difficult, since transduced CD62L⁺ cells might have turned negative for CD62L when gene expression becomes detectable. Yet, T cells transduced with 62L-LV contained significantly higher proportions of CD62L⁺CAR T cells than those generated with VSV-LV. While this already indicated that CD62L was used as entry receptor, we provide further evidence for its selectivity from transduction of engineered CD62L expressing cells as well as vector particle binding assays to primary T cells. Binding of 62L-LV to primary T lymphocytes was specifically blocked by the parental CD62L-specific antibody from which the targeting domain of 62L-LV was derived.

An interesting finding of our study was that 62L-LV particles were not blocked by shed CD62L. This was not expected, as it is known that binding capacities of CD62L to target molecules are retained after cleavage. Various reasons might be causative for this finding. The concentration of sCD62L in cell culture supernatants were lower (50 ng/mL) than those in serum of healthy individuals ($0.8 - 2.3 \mu g/mL$). In addition, sCD62L is known to aggregate which further reduces the amounts of molecules available for binding of 62L-LV. Even more relevant, it has been suggested that sCD62L is conformationally different from the membrane-associated full-length CD62L as a monoclonal antibody directed against an epitope in the EGF-like domain of CD62L was able to bind to the cell-surface associated CD62L but not the soluble form. The same may hold true for the 145/15 antibody. As a consequence, 62L-LV would be specific for CD62L but not the conformational different sCD62L. Regardless of the exact mechanism, we have proven that 62L-LV transduces T lymphocytes also in presence of sCD62L.

Currently approved CAR T cell products available on the US and EU market include Yescarta, Kymriah, Abecma, Tecartus and Breyanzi. Genetic modification of those products is accomplished by transduction with VSV-LV or γ -retroviral vectors. According to information provided on the companies' homepages, between 2-5 weeks are required for CAR T cell production and release. To reduce production times, shorter T cell cultivation and expansion could be beneficial. In this regard, we show here that CAR T cells generated

within three days of *ex vivo*handling control the tumor burden in a mouse model. This result is well in line with the previous observation of Ghassemi and colleagues, who have shown that functional CAR T cells cannot be only generated within three days, but also outperform conventionally generated CAR T cells in xenogeneic mouse tumor models. In difference to the published results, we stimulated our cells with IL-7 and IL-15 instead of IL-2, activated the PBMC for only two days with α CD3 and α CD28 and administered the cells already 24 hours after vector incubation. Additionally, using 62L-LV less differentiated T cells were directly targeted. It remains to be analyzed in more sophisticated mouse models whether targeting these cells provides a survival-advantage over VSV-LV incubated CAR T cells.

While shortening the manufacturing time for CAR T cells appears feasible and desirable, certain safety concerns arise with this procedure. During conventional CAR T cell manufacturing, transduced cells undergo several washing and expansion steps reducing the amounts of residual vector particles to negligible concentrations. In contrast, it can be assumed that particle uptake and gene transfer are not completed for CAR T cell products injected as early as 24 or 48 hours after vector incubation. Vector particles still bound to the T cells may transduce other cells upon infusion. This risk is expected to be higher for VSV-G pseudotyped vectors that have a broad cell tropism. That such a scenario can be fatal was demonstrated 2018 in a clinical trial investigating the CAR T cell product Kymriah. In this trial, an accidental transfer of a CD19-CAR into a single leukemic cell during manufacturing led to relapse and death of a patient. Causative for this event was that a CAR construct present in tumor cells can bind in cis to the CAR specific epitope on the surface of the tumor cell, in this case CD19, mask the epitope from recognition by CAR T cells, conferring resistance to the CAR T cell product and enabling its proliferation. In contrast to VSV-LV, RT-LVs, like 62L-LV, have a more restricted tropism which is controlled by the specificity of the used targeting domain. Theoretically, 62L-LV might bind and transduce all kinds of CD62L⁺ cells, like B lymphocytes, neutrophils, monocytes, eosinophils, hematopoietic progenitor cells, immature thymocytes and a subset of NK cells. Yet. it has to be assessed whether those cells will be modified by 62L-LV in vivo and what consequence the potential CAR expression in these CD62L-positive cell types could have. Importantly, it has to be ensured that tumor cells do not express CD62L. In order to reduce this potential safety concern, the exact time-point of completed transduction after short-term incubation should be investigated and additional washing steps could be implemented to remove residual particles from the cells prior to adoptive transfer.

Taken together, the newly established 62L-LV has shown great potential for the generation of less differentiated CAR T cells without the need of prior or later T cell subtype selection. It is thus a suitable alternative to VSV-G pseudotyped LV vectors. One immediate application may be its use for short-term generated CAR T cells within few days, which may substantially simplify CAR T cell production. Although promising, this approach will need further investigation with regard to safety concerns and scalibility of receptor targeted lentiviral vector production before implemented into clinical studies.

Material and Methods

Ethics Statement

Work performed with primary cells isolated from blood donations was invariably obtained from anonymous donors that had provided written informed consent in full compliance with the requirements of the Ethics Committee of the University Hospital Frankfurt, Germany.

Cell lines and primary cells

HEK293T (ATCC CRL-11268), HT1080 (ATCC CCL-121) and HT1080_{α Htc} cells were cultivated in DMEM (Sigma-Aldrich, Munich, Germany) supplemented with 10% fetal calf serum (FCS; Biochrom, Berlin, Germany) and 2 mM L-glutamine (Sigma-Aldrich, Munich, Germany). Culture medium of HT1080_{α Htc} cells was furthermore supplemented with 1.2 mg/mL G418 (Thermo Fisher Scientific, Darmstadt, Germany). The

cell line HT1080_{CD62L} was generated by LV transduction of the parental HT1080 cell line with LV particles packaging a construct encoding a spleen focus-forming virus (SFFV) promoter, the gene encoding CD62L (UniProt: P14151), an internal ribosome entry site (IRES) element followed by a puromycin resistance gene and a woodchuck posttranscriptional regulatory element (WPRE) (transfer plasmid: pS-CD62L-IPW). Transduced cells were selected using puromycin for 2 weeks. Nalm-6-eBFP-Luc (kindly provided by Prof. Helen Fielding, University College of London), further on called Nalm6, were grown in complete Roswell Park Memorial Institute (RPMI) medium (RPMI 1640, Biowest), supplemented with 10% FCS and 2 mM L-glutamine.

Human PBMC were isolated from fresh blood of healthy donors or buffy coats purchased from the German blood donation center (DRK-Blutspendedienst Hessen, Frankfurt) and cultured in T cell medium (TCM) consisting of RPMI 1640 supplemented with 10% FCS, 2 mM L-glutamine, 0.5% streptomycin/penicillin, 25 mM HEPES (Sigma-Aldrich, Germany), 25 U/mL IL-7 and 50 U/mL IL-15 (all cytokines from Miltenyi Biotec, Germany). For activation, 1×10^7 PBMC per 6-well were cultured in TCM supplemented with 3 µg/mL anti-CD28 antibody (clone 15E8, Miltenyi Biotec, Germany) for 48 hours. 6-well plates for activation were pre-coated with 1 µg/mL anti-CD3 antibody (clone OKT3, Miltenyi Biotec, Germany).

Generation of CD62L-targeted envelope constructs

To generate the CD62L targeting constructs, the coding sequences of the variable light chain (VL) and heavy chain (VH) of the parental CD62L-specific monoclonal antibody 145/15 were synthesized de novo (GeneArt, Thermo Fisher Scientific) and cloned into the backbone encoding the modified Nipah virus (NiV) glycoprotein G with and without glycine-serine linker (pCG- $G_{NiV}\Delta34$ mut-His and pCG- $G_{NiV}\Delta34$ mut-L3-His) or the modified measles virus (MV) hemagglutinin protein (pCG- $H_{MVnse}\Delta18$ mut-L3-His) via digestion with *Sfi* I and *Not* I. DNA sequences were verified by standard sequencing technologies prior to use in LV production.

LV production and characterization

Vector particles were generated by transient transfection of HEK-293T cells using polyethylenimine (PEI) and second generation packaging plasmids as described in detail by Weidner and colleagues. In brief, one day before transfection, $1.5-2 \times 10^7$ cells were seeded into a T175 flask. In total, 35 µg DNA was added to 2.3 mL of DMEM without additives and combined with 2.2 mL DMEM containing 140 µL of 18 mM PEI solution. The transfection solution was mixed and incubated for 20 min at room temperature. The cell medium was replaced by 10 mL DMEM supplemented with 15% FCS and 3 mM L-glutamine, before the transfection solution was added to HEK-293T cells. 4-6 hours later the medium was replaced by DMEM with 10% FCS and 2 mM L-glutamine. Two days after transfection, the cell culture supernatant was collected and filtrated. Released vector particles were concentrated over a 20% sucrose cushion at 4500xg for 24 hours, before supernatant was discarded and pellets were resuspended in 60 μ L PBS per T175 flask. The used transfer plasmid encoded a second generation CD19-CAR in conjunction with Δ LNGFR. Notably, based on the coexpression of Δ LNGFR and the CAR construct, detection of Δ LNGFR can be used as surrogate marker for the expression of CAR molecules on the cell surface. Plasmid ratios for the generation of NiV-based and MVbased RT-LV particles as well as particles pseudotyped with VSV-G were described previously and can be found in the supplemental table 1. If not otherwise specified, all concentrated vector stocks were titrated on $HT1080_{\alpha HLc}$ cells as described previously using a LNGFR specific antibody for detection. LV particle yields were determined by nanoparticle tracking analysis or p24-specific enzyme-linked immunosorbent assay (HIV type 1 p24 Antigen ELISA; ZeptoMetrix Corporation) according to the manufacturer's instructions and calculated as described.

Transduction of cell lines and primary cells

Parental HT1080, HT1080_{α Huz}, and HT1080_{CD62L} cells were seeded at 8x10³ cells per 96-well and incubated with serial dilutions of vector stocks. Transgene expression was analyzed 72 to 96 hours later by flow cytometry. Activated PBMC were seeded at 4x10⁴ or 8x10⁴ cells per 96-well, respectively, in TCM medium before CD62L-LV (5 µL or 10 µL) or VSV-LV (0.05 µL or 0.5 µL) were added. Where indicated, CD62L-LV transduction of PBMC was carried out in presence of Vectofusin-1 (Miltenyi Biotec, Germany) as described previously. Cells were centrifuged at 850g, 32°C for 90 minutes, followed by addition of TCM. Medium was replenished every 2 to 3 days. Transgene expression was assessed by flow cytometry.

Quantification of shed CD62L by ELISA

Activated PBMC of three donors were cultured without medium change or cell passaging for up to 10 days. At the indicated time points, cell suspension was collected and centrifuged for 5 minutes at 5,000 rpm and either stored at -80°C or 4°C. Concentration of sCD62L in supernatant was determined by ELISA (Human L-Selectin/CD62L DuoSet ELISA, R&D Systems) following the manufacturer's protocol with the exception that heat inactivated FBS was used instead of inactivated goat serum. Quantification of the fluorescent signals was performed with a microplate reader (EmaxPlus, Molecular Devices).

Blocking assay with shed CD62L or antibodies

For the blocking assay with antibodies, $4x10^4$ activated PBMC were preincubated with the indicated concentrations of a CD62L-specific antibody (clone 145/15, Miltenyi Biotec) or a CD45-specific antibody (clone 5B1, Miltenyi Biotec) either conjugated to the fluorophore phycoerythrin (PE)-Vio770 or to biotin for 1 h at 4°C. Before and after antibody incubation, cells were washed twice with wash buffer (phosphate-buffered saline (PBS) supplemented with 2% FBS and 0.1% NaN₃). Afterwards, either 10 µL of 62L-LV or PBS were added to cells pre-incubated with biotin conjugated antibodies, while PBS was added to cells pre-incubated with fluorophore-conjugated antibodies. All samples were incubated at 4°C for 30 min. Cells pre-incubated with biotin conjugated antibodies were further stained with a PE-labeled anti-LNGFR antibody (clone ME20.4-1.H4, Miltenyi Biotec). After two additional washing steps, antibody and vector bound cells were determined by flow cytometry analysis respectively.

For the sCD62L blocking assays, 10 μ L of 62L-LV or VSV-LV vector particles were pre-incubated with 90 μ L fresh or frozen supernatant containing sCD62L derived from six days of PBMC culture or TCM only for 1 h at 4°C. Vector/sCD62L-containing supernatant was then added to 4x10⁴ activated PBMC of various donors in 96-wells. Staining for vector bound cells was performed after an incubation for 30 minutes at 4°C by flow cytometry detecting Δ LNGFR.

Animal experiment

All animal experiments were conducted in accordance with the German Animal Protection Law and the respective European Union guidelines.

For short-time generation of CAR T cells, 1.8×10^6 activated PBMCs were seeded in 600 µL TCM per 24 well, mixed with 30.6 µL 62L-LV (equals MOI of 1.3 or $^{-}4 \times 10^{10}$ particles) or VSV-LV (equals an MOI of 8.8 or $^{-}3 \times 10^{10}$ particles) or equal volume of PBS and centrifuged for 90 min at 850g, 32°C before addition of TCM to a total volume of 1.2 mL per well. 24h after vector incubation, cells were harvested and washed 2x with PBS prior in vivo application. NSG mice (NOD.Cg.Prkdc^{scid}IL2rg^{tmWjl}/SzJ, Jackson Laboratory) were intravenously (i.v.) injected with 2×10^6 vector bound cells or 1.4×10^6 PBS treated cells. Three days later, 5×10^5 Nalm-6 were injected i.v. and tumor growth was followed by bioluminescence imaging (BLI). This was performed by injecting D-luciferin (Perkin Elmer) intraperitoneally at 150 µg/kg body weight and imaging luciferase signals 10 minutes after injection using the IVIS Imaging System (Perkin Elmer). CAR T cell

engraftment was monitored through regular, blood drawings. Mice were checked regularly for health status and tumor load by IVIS. All mice were sacrificed on day 17 for final analysis of blood and organs (spleen, bone marrow and liver).

Collected blood and organs were prepared to a single cell suspension and analyzed by flow cytometry analysis. Blood was washed with PBS prior and after erythrocyte lysis using BD Pharm Lyse buffer (BD Bioscience). Spleens were minced through a 70 μ m cell strainer to obtain a single cell solution and proceeded with erythrocyte lysis. Bone marrow was harvested through centrifugation of long bones cut open with a scalpel in pierced 0.5 mL tubes at 8000 rpm for 5 min. Bone marrow cells were then washed with PBS and singularized through a 70 μ m cell strainer and erythrocyte lysis was performed. Liver cells were isolated using the mouse liver dissociation kit (Miltenyi Biotec) according to the manufacturer's instruction, washed with PBS and erythrocytes were lysed.

Flow cytometry

Flow cytometry analysis was performed using MACSQuant Analyzer 10 (Miltenyi Biotec, Bergisch Gladbach, Germany) or LSR Fortessa (BD Biosciences) flow cytometers. Data were analyzed by FCS Express 6 (De Novo Software, Glendale, CA, USA) or FlowJo 7 (BD Biosciences). Before and after staining with fluorescently labelled antibodies, cells were washed twice with wash buffer. Before measurement cells were fixed by addition of PBS supplemented with 1% formaldehyde. To determine the percentage of transduced cells or cell-bound vector particles, staining of up to 1×10^5 cells was performed. The reporter protein Δ LNGFR, which is co-expressed with the CD19-CAR, was detected using the anti-LNGFR-PE antibody. PBMC were further stained with the fixable viability dye eFluor780 (Life Technologies, Darmstadt, Germany), according to the manufacturer's instructions or with 7-AAD to detect viable cells. To further characterize the PBMC, cells were stained in addition with a CD4-specific antibody (clone VIT4) labeled with VioGreen or PE-Vio770 and a CD8-specific antibody (clone BW135/80) labeled with allophycocyanin (APC) or APCVio770 and if indicated with a CD62L-specific antibody (clone 145/15) labeled with PEVio770. All antibodies were from Miltenyi Biotec (Bergisch Gladbach, Germany). The following antibodies were used for flow cytometry analysis of the *in vivo* experiment: CD45-BV510 (clone 2D1, BioLegend), CD3-BV605 (clone HIT3a, BD Bioscience), CD8-BV786 (clone RPA-T8, BD Bioscience), LNGFR-PE (clone ME20.4-1.H4, Miltenvi Biotec), CD4-PE-CF594 (clone RPA-T4, BD Bioscience), CD19-Alexa Fluor 700 (clone HIB19, Thermo Fisher), eFluor780 (eBioscience).

Statistical Analysis

Statistical analyses were performed with Prism 7 software (GraphPad). Tests for statistical significance used the unpaired or paired two-tailed Student's t test, one-way ANOVA (Dunnett multiple comparisons test), two-way ANOVA (Dunnett or Turkey multiple comparisons test) or Fisher's least significant difference (LSD) test as indicated. Statistical differences in experiments were considered significant at p < 0.05.

Acknowledgment

We thank Shiwani Agarwal for the help in designing the flow cytometry panel and assistance in the animal work. This work was supported by grants from the European Union (Horizon 2020 Framework Programme (H2020), CARAT [667980]) to CJB.

Conflict of Interest Statement

CJB, JH, FBH, LK and TS are listed as an inventor on a patent describing 62L-LV. TS is a full time employee of Miltenyi Biotec GmbH. All other authors declare no conflict of interest.

Author contributions

LK and TK designed and performed experiments. LK, TK, NH, FBT, JH and CJB evaluated data. TS contributed protocols and reagents and to writing of the manuscript. CJB and JH conceived and designed the study, acquired grants, supervised work and wrote the manuscript.

Data availability statement

All datasets on which the conclusions of the paper rely are presented in the main manuscript or in the supplemental information.

Figure Legends

Figure 1: Basic characterization of 62L-LV.

A) Physical properties of 62L-LV vector stocks. Three independently produced 62L-LV stocks were analyzed for size (left panel) and for particle concentration (right panel) by nanoparticle tracking analysis (filled bar; technical triplicates) or p24-ELISA (open bar, biological replicates). Means and standard deviations (SD) are depicted.**B**) 62L-LV stocks were titrated on HT1080_{α Htc}cells or activated human PBMC. Individual results and means with standard error (SEM) are plotted. Statistical significance was determined by using unpaired t-test. **C**) Target and non-target HT1080 cells were incubated with 2.5 μ L 62L-LV stock for 4 days or left untransduced. Antibody staining for Δ LNGFR allowed detection of transduced cells by flow cytometry. Left panel: Representative dot plots of one vector stock. Right panel: Percent Δ LNGFR expressing HT1080 cells after transduction with seven different vector stocks. Dashed lines indicate baseline Δ LNGFR levels on each individual cell line. Individual results as well as means with SD are plotted. Statistical testing was performed by using ordinary 1-way ANOVA. WT = parental HT1080 cells.

Figure 2: CAR gene delivery to primary lymphocytes by 62L-LV

Activated PBMC were incubated with 62L-LV (blue dots) or VSV-LV (orange dots). A) Transduction rates in the presence (+V1) or absence (-V1) of Vectofusin-1. Left panel: Representative dot plots of 62L-LV transduced PBMC pre-gated for CD3+ cells. Right panel: Results for PBMC from seven different donors in four independent experiments analyzed 9 - 12 days post-transduction. For VSV-LV, no V1 was applied. Individual results and means with standard deviation (SD) are plotted. Statistical analysis was performed by using paired t-test for the comparison of 62L-LV +/-V1 and by using unpaired t-test for the comparison of 62L-LV and VSV-LV. B) The total percentage of Δ LNGFR+ cells expressing CD62L is displayed for the CD4+ (left) and CD8+ (right) fractions. Transduction was performed in absence of V1 for 62L-LV and VSV-LV, respectively. Cells transduced with either vector were tested for significant differences at each analysis time point individually by Fisher's least significant difference (LSD) test. Mean with standard error (SEM) of 8 individual experiments is plotted.

Figure 3: Selectivity in 62L-LV binding to primary T lymphocytes.

Activated PBMC incubated either with the CD62L-specific antibody (blue bars) or with the CD45-specific antibody (grey bars) at the indicated concentrations before PBS (open bars) or 62L-LV vector particles (filled bars) were added for 30 min at 4°C. **A**) Fluorophore-labelled α CD62L and α CD45 antibodies were used to determine the staining intensity of CD62L and CD45 on activated PBMC at the indicated concentrations by flow cytometry. Mean fluorescent intensities (MFI) are shown. **B**) PBMC were pre-incubated with biotin-labelled antibodies before addition of 62L-LV particles. After vector incubation, cells were stained with fluorophore coupled α CD3 and α LNGFR antibodies to allow detection of vector bound T cells by flow cytometry. Background MFI (dashed line) is determined from samples incubated with PBS (w/o) instead of 62L-LV accumulated for all antibody concentrations. Means of MFI and standard deviations (SD) are depicted. Statistical testing was performed by using 2-way ANOVA.

Figure 4: Shed CD62L does not influence vector binding.

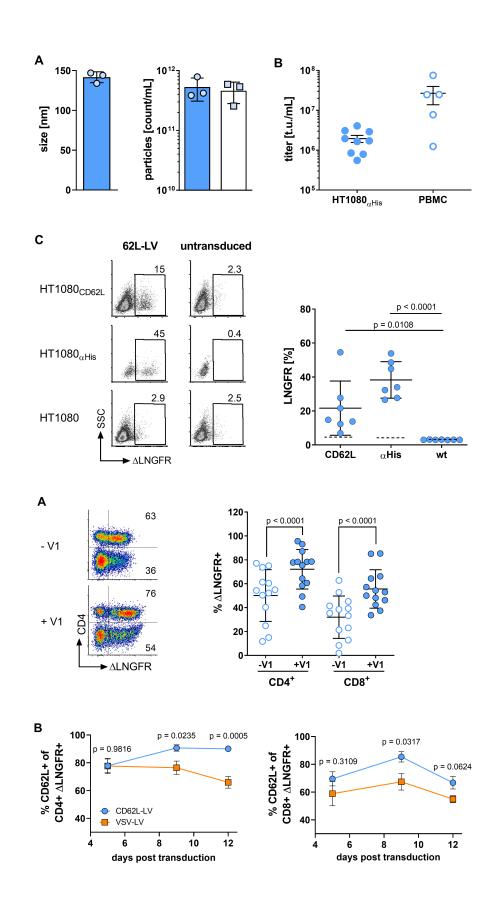
A) Accumulation of sCD62L in the supernatant of PBMC. Frozen PBMC were thawed, activated and cultivated in presence of IL-7 and IL-15. The complete supernatant of one well was collected at the indicated day and used for sCD62L quantification (left panel). The amounts of sCD62L present in three independent cultures at day 6 are shown in the right panel. Individual results, means and standard deviation (SD) are depicted. **B**) 62L-LV (blue) or VSV-LV (orange) particles were incubated with fresh or frozen supernatant containing sCD62L (day 6 harvest) or cell medium (TCM) only. Mixture of vector stock and supernatant was incubated with activated PBMC for 30 min at 4°C. Flow cytometry was performed analyzing content of vector bound T cells by staining with fluorophore coupled α CD3 and α LNGFR antibodies. Dot plots of vector bound T cells are depicted in the right panel. Percentage of vector bound cells is indicated. Δ LNGFR intensity [MFI] of vector bound cells in 3 - 10 independent experiments is shown in the left panel. Individual results and means with SD are plotted. Statistical testing was performed by using 2-way ANOVA.

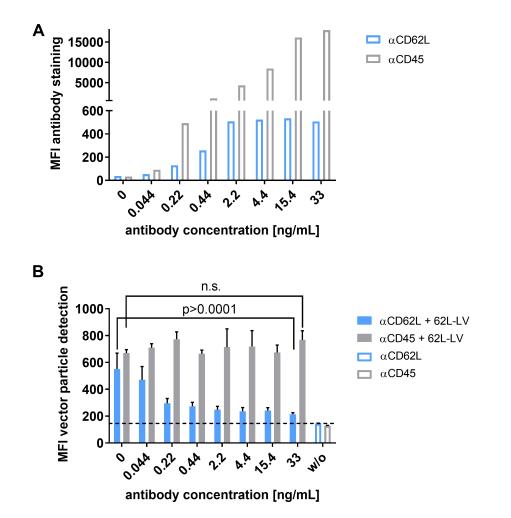
Figure 5: Antitumoral activity of CAR T cells generated with 62L-LV.

A) Experimental setting. PBMC were activated for two days prior to 24h incubation with 62L-LV, VSV-LV or PBS (control) and injected i.v. into NSG mice. Nalm6 cells were injected at day 4 post adoptive cell transfer and their growth was followed by bioluminescence imaging (BLI).B) Monitoring for tumor load by BLI at the indicated days after adoptive cell transfer. Ventral images of each mouse are depicted.C) Total body flux quantified at the indicated time points for the 62L-LV group (blue), the VSV-LV group (orange) and the control (grey). Mean with standard error (SEM) is plotted. Dotted line represents background signal of mice without imaging substrate. Ordinary 1-way ANOVA was used to determine statistics. D) Cells isolated from blood and organs of each mouse were analyzed by flow cytometry for viable, CD45 negative, CD19 and EBFP double-positive Nalm6 cells. The percentage of Nalm6 positive cells of all viable cells is depicted. Individual results and means with standard error are plotted.

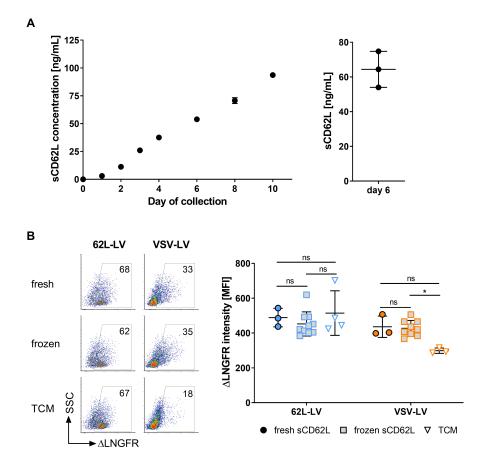
Φιγυρε 6: Εξπρεσσιον οφ $\Delta \Lambda N \Gamma \Phi P +$ ιν ηυμαν $\Delta 4^+$ ορ $\Delta 8^+$ T ςελλς

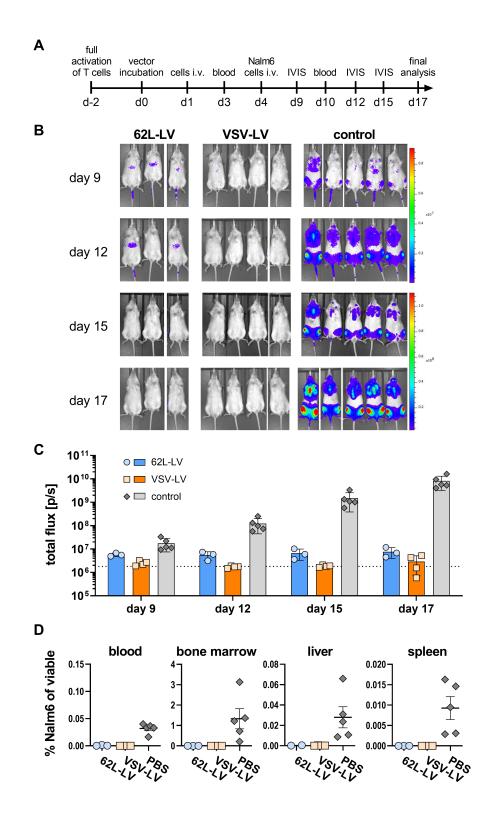
A) Presence of Δ LNGFR+ cells on human CD4⁺ or CD8⁺ T cells in blood determined by flow cytometry on day 3, 10 and 17 of the experiment. Gating on viable human CD45⁺, CD3⁺ and respective lineage marker positive cells was performed. Only data with at least 20 events in CD4⁺ or CD8⁺ T cell gate are shown. Mean with standard error (SEM) are depicted. **B-E**)Presence of human CD45⁺ cells (left), Δ LNGFR+ human CD4⁺ (middle) or Δ LNGFR+ human CD8⁺T cells (right) in spleen (**B**), blood (**C**), bone marrow (**D**) and liver (**E**) as determined by flow cytometry at final analysis. Individual results and mean with standard deviation (SD) are depicted. Unpaired t-tests were performed to determine statistics.





/doi.org/10.22541/au.166429989.90389382/v1 —





5
ij.
pre
0
ay b
ma
ata
Dai
ewec
iev
revi
36I'
õ.
en
ã,
ot
as r
has
pg
nt a
epi
d
S a
This
1
E
82
389382
338
6.6
9989
342.96
64
10
au
=
2254
10.22
org/
doi.6
ttps://
https:
Ē,
ht
- P
ion h
ission. — h
ermission. — h
permission h
ermission. — h
thout permission. — h
without permission. — h
without permission. — h
thout permission. — h
use without permission. — h
No reuse without permission. — h
d. No reuse without permission. — h
d. No reuse without permission. — h
d. No reuse without permission. — h
erved. No reuse without permission. — h
reserved. No reuse without permission. — h
rights reserved. No reuse without permission. — h
rights reserved. No reuse without permission. — h
tts reserved. No reuse without permission. — h
rights reserved. No reuse without permission. — h
rights reserved. No reuse without permission. — h
/funder. All rights reserved. No reuse without permission. — h
or/funder. All rights reserved. No reuse without permission. — h
thor/funder. All rights reserved. No reuse without permission. — h
author/funder. All rights reserved. No reuse without permission. — h
the author/funder. All rights reserved. No reuse without permission. — h
author/funder. All rights reserved. No reuse without permission. — h
the author/funder. All rights reserved. No reuse without permission. — h
the author/funder. All rights reserved. No reuse without permission. — h
the author/funder. All rights reserved. No reuse without permission. — h
ght holder is the author/funder. All rights reserved. No reuse without permission. — h
yright holder is the author/funder. All rights reserved. No reuse without permission. h
ght holder is the author/funder. All rights reserved. No reuse without permission. — h
copyright holder is the author/funder. All rights reserved. No reuse without permission. — h
ppyright holder is the author/funder. All rights reserved. No reuse without permission. — h
The copyright holder is the author/funder. All rights reserved. No reuse without permission. — h
— The copyright holder is the author/funder. All rights reserved. No reuse without permission. — h
The copyright holder is the author/funder. All rights reserved. No reuse without permission. — h
2022 - The copyright holder is the author/funder. All rights reserved. No reuse without permission. $- h$
2022 — The copyright holder is the author/funder. All rights reserved. No reuse without permission. — h
2022 - The copyright holder is the author/funder. All rights reserved. No reuse without permission. $- h$
7 Sep 2022 — The copyright holder is the author/funder. All rights reserved. No reuse without permission. — h
7 Sep 2022 — The copyright holder is the author/funder. All rights reserved. No reuse without permission. — h
7 Sep 2022 — The copyright holder is the author/funder. All rights reserved. No reuse without permission. — h
horea 27 Sep 2022 — The copyright holder is the author/funder. All rights reserved. No reuse without permission. — h
Authorea 27 Sep 2022 — The copyright holder is the author/funder. All rights reserved. No reuse without permission. — h
horea 27 Sep 2022 — The copyright holder is the author/funder. All rights reserved. No reuse without permission. — h

